MOLECULAR AND CELLULAR BIOLOGY, June 2009, p. 2982–2996 Vol. 29, No. 11
0270-7306/09/$08.00+0 doi:10.1128/MCB.00042-09

A Mouse *PRMT1* Null Allele Defines an Essential Role for Arginine Methylation in Genome Maintenance and Cell Proliferation▽

Zhenbao Yu,[1] Taiping Chen,[2] Josée Hébert,[3] En Li,[2] and Stéphane Richard[1]*

Terry Fox Molecular Oncology Group and Bloomfield Center for Research on Aging, Segal Cancer Centre, Lady Davis Institute for Medical Research, Sir Mortimer B. Davis Jewish General Hospital, and Departments of Oncology and Medicine, McGill University, Montréal, Québec H3T 1E2, Canada[1]; Epigenetics Program, Novartis Institutes for Biomedical Research, 250 Massachusetts Avenue, Cambridge, Massachusetts 02139[2]; and Leukemia Cell Bank of Quebec and Division of Hematology, Maisonneuve-Rosemont Hospital, Montreal, Quebec, Canada, and Department of Medicine, Université de Montréal, Montreal, Quebec H3C 3J7, Canada[3]

Received 10 January 2009/Returned for modification 19 February 2009/Accepted 9 March 2009

Protein arginine methyltransferase 1 (PRMT1) is the major enzyme that generates monomethylarginine and asymmetrical dimethylarginine. We report here a conditional null allele of *PRMT1* in mice and that the loss of PRMT1 expression leads to embryonic lethality. Using the Cre/lox-conditional system, we show that the loss of PRMT1 in mouse embryonic fibroblasts (MEFs) leads to the loss of arginine methylation of substrates harboring a glycine-arginine rich motif, including Sam68 and MRE11. The loss of PRMT1 in MEFs leads to spontaneous DNA damage, cell cycle progression delay, checkpoint defects, aneuploidy, and polyploidy. We show using a 4-hydroxytamoxifen-inducible Cre that the loss of PRMT1 in MEFs leads to a higher incidence of chromosome losses, gains, structural rearrangements, and polyploidy, as documented by spectral karyotyping. Using PRMT1 small interfering RNA in U2OS cells, we further show that PRMT1-deficient cells are hypersensitive to the DNA damaging agent etoposide and exhibit a defect in the recruitment of the homologous recombination RAD51 recombinase to DNA damage foci. Taken together, these data show that PRMT1 is required for genome integrity and cell proliferation. Our findings also suggest that arginine methylation by PRMT1 is a key posttranslational modification in the DNA damage response pathway in proliferating mammalian cells.

Methylation of arginine residues is one of many posttranslational modifications of eukaryotic proteins (7). Arginine methylation is catalyzed by a family of enzymes named protein arginine methyltransferases (PRMTs). PRMTs catalyze the direct transfer of a methyl group from *S*-adenosyl-L-methionine to one or two of the guanidino nitrogen atoms in arginine (7). In higher eukaryotes, there are 11 PRMTs classified into two groups according to their substrate specificity and reaction products (6). Type I enzymes, including PRMT1 (39), PRMT3 (54), CARM1 (16), PRMT6 (25), and PRMT8 (37), catalyze the formation of N^G-monomethylarginine and asymmetric N^G,N^G-dimethylarginine, while type II enzymes, including PRMT5 (45), and PRMT7 (41), catalyze the formation of N^G-monomethylarginine and symmetric N^G,N'^G-dimethylarginine. PRMT2 (49) has no detectable activity, and the activity of PRMT9 has not been determined (6). FBXO10 and FBXO11 were proposed as PRMT10 and PRMT11 (19).

The *PRMT1* and *PRMT3* genes have been targeted in mouse embryonic stem (ES) cells using gene-trapping strategies (44, 53). The targeted alleles in both cases result in hypomorphic alleles with ~5% residual PRMT1 and PRMT3 expression, respectively (20, 53). Mice homozygous for the PRMT1 gene-trap hypomorphic allele die at around embryonic day 6.5 (E6.5). ES cells were isolated that are homozygous for the PRMT1 hypomorphic allele, and these cells harbor numerous hypomethylated proteins (44), including Sam68 (20), MRE11 (12), histone H4 (52, 61), and hnRNPK (43). PRMT3 null mice have retarded growth during gestation but develop normally thereafter. Mouse embryonic fibroblasts (MEFs) derived from these PRMT3 cells harbor hypomethylated ribosomal protein rpS2 (53).

PRMT2 and CARM1 null mice have been generated by gene targeting using homologous recombination (HR). PRMT2 null mice are viable with no gross abnormalities (68). However, the *PRMT2*$^{-/-}$ MEFs have elevated NF-κB activity and decreased susceptibility to apoptosis (27). *PRMT2*$^{-/-}$ MEFs also have an earlier S phase entry by bromo-2′-deoxyuridine (BrdU) staining, but the growth profiles are similar to those of wild-type MEFs (68). *CARM1*$^{-/-}$ mice survive to birth but die perinatally (66). *CARM1*$^{-/-}$ mice have a defect in thymocyte maturation at an early progenitor stage (35) and an adipogenesis defect (65). CARM1 serves as a coactivator for numerous transcription factors, including nuclear receptors, p53, NF-κB and MEF2C (6).

PRMT1 is the predominant type I PRMT in mammalian cells, responsible for at least 85% of all arginine methylation reactions in human cells (55). *Saccharomyces cerevisiae* without the PRMT1 homolog (*hmt1*/*Rmt1*) are viable, mislocalize cellular proteins (50) and harbor defects in maintaining silent chromatin (4, 69). PRMT1 catalyzes substrate dimethylation in a partially processive manner (42) and oligomerizes into ring-like structures (70). A large number of PRMT1 substrates are

* Corresponding author. Mailing address: Segal Cancer Centre, 3755 Côte Ste.-Catherine Road, Montréal, Québec H3T 1E2, Canada. Phone: (514) 340-8260. Fax: (514) 340-8295. E-mail: stephane.richard@mcgill.ca.

▽ Published ahead of print on 16 March 2009.

known, and its preferred methylation sites are arginines that lie within glycine- and arginine-rich (GAR) sequences that include multiple arginines in RGG or RXR contexts (7). As such, antibodies have been generated that recognize methylated GAR regions and are good indicators of PRMT1 activity within the cell (10). PRMT1 substrates that lack a GAR motif have been identified including, PGCα (56), the estrogen receptor (38), and FOXO transcription factors (67). As reflected by the diversity of its substrates, PRMT1 is implicated in the regulation of a plethora of cellular processes. For example, PRMT1 is implicated in the transcriptional coactivation of nuclear hormone receptors because it methylates histone H4 (52, 61) and thereby facilitates histone acetylation and chromatin remodeling (3). In addition, PRMT1 methylates the RNA-binding protein Sam68 (20) and the DNA damage response (DDR) proteins MRE11 (11, 21) and 53BP1 (1, 13). MRE11 forms a complex with RAD50 and NBS1 and is referred to as the MRN complex (48). More recently, PRMT1 has been shown to regulate the cytoplasmic signaling function of the estrogen receptor α (38). In addition to its numerous cellular function, the PRMT1 activity is dysregulated in cancer (7). PRMT1 is aberrantly expressed in prostate cancer and likely contributes to the proliferative capacity of prostate cancer cells through its ability to act as a transcriptional coactivator for the androgen receptor (7). Moreover, the knockdown of PRMT1, or its substrate Sam68, suppressed mixed lineage leukemia-mediated transformation (18).

In the present study, we report the generation of the first *PRMT1* null allele in mice. We show that the MEFs lacking PRMT1 exhibit spontaneous DNA damage, cell cycle delays, checkpoint activation defects after DNA damage, polyploidy, and chromosome instability. Moreover, PRMT1 knockdown U2OS cells are hypersensitive to etoposide and have an impaired ability to recruit the RAD51 recombinase to DNA damage sites. These findings demonstrate that arginine methylation by PRMT1 plays a key role in genome maintenance and the DDR pathway.

MATERIALS AND METHODS

Reagents and antibodies. BrdU, 4-hydroxytamoxifen (OHT), and Polybrene were purchased from Sigma (St. Louis, MO). Mouse anti-γH2AX monoclonal antibody, rabbit anti-phospho-histone H3-Ser10, anti-Sam68, anti-PRMT1, anti-PRMT5, anti-PRMT7, and ASYM24 antibodies were obtained from Millipore (Billerica, MA). Rabbit anti-MRE11 and anti-53BP1 antibodies were from Novus Biologicals (Littleton, CO). Rabbit anti-RAD51 antibody was from Santa Cruz Biotechnology (Santa Cruz, CA). Anti-CARM1 was generated as described previously (35). The anti-PRMT6 antibody was purchased from IMGENEX (San Diego, CA). ASYM25b antibody was generated in rabbits using asymmetrically dimethylated GAR motif as described previously (10). Propidium iodide (PI) and Alexa Fluor 488-conjugated goat anti-rabbit and anti-mouse immunoglobulin G (IgG) antibodies were from Invitrogen (Carlsbad, CA). Fluorescein isothiocyanate (FITC)-conjugated mouse IgG antibody was obtained from Sigma. FITC-conjugated mouse anti-BrdU monoclonal antibody was from BD Biosciences, Pharmingen (San Diego, CA). Immunoprecipitations and immunoblotting were performed as previously described (9).

Cell culture, retrovirus infection, and transfection. We constructed the PRMT1 conditional allele in mice essentially as described previously (17, 33). The sequenced plasmids were linearized and electroporated into 129/Sv ES cells. Three independent ES cell clones with homologous integration at the targeting site were injected into C57BL/6J blastocysts, and chimeras were obtained. These chimeras were subsequently crossed with C57BL/6J females, and the heterozygous mice with successful germ line transmission of the targeted allele were crossed with C57BL/6J mice expressing Flp recombinase to remove the neomycin resistance cassette, resulting in a floxed allele ($PRMT^{FL/+}$). To disrupt PRMT1, heterozygous $PRMT1^{FL/+}$ mice were crossed with Zp3-Cre mice, resulting in a heterozygous deletion ($PRMT1^{+/-}$) of the methyltransferase domain for PRMT1. We bred the $PRMT1^{FL/+}$ mice with the $PRMT1^{+/-}$ mice to generate $PRMT1^{FL/-}$ MEFs from E14.5 embryos. Spontaneously immortalized MEFs were created according to standard 3T3 protocol. U2OS cells were obtained from American Type Culture Collection (Manassas, VA). All cells were grown in Dulbecco modified Eagle medium containing 10% bovine calf serum.

Retroviral vectors encoding green fluorescent protein (GFP), GFP-CRE fusion protein, or CRE and hygromycin marker (hygro-Cre) were from Guy Sauvageau (Institut de Recherche en Immunologie et en Cancérologie, Montréal, Québec, Canada). Viral particles were produced using an ecotropic packaging system and used for infection of primary or immortalized MEFs as described previously (40).

Immortalized MEFs were transfected by a plasmid DNA encoding estrogen receptor-CRE fusion protein (ER-CRE) and blasticidin selection marker (pCAG-IREShlast-ER-CRE) (17) using Lipofectamine 2000 (Invitrogen) according to the manufacturer's instructions. Stable cell lines were selected with 3 μg of blasticidin/ml, and a few single clones were collected. The cells were treated with the estrogen receptor ligand, OHT, to induce relocalization of the ER-CRE fusion protein. OHT was removed from the culture medium 2 days before performing a phenotype analysis. Human osteosarcoma U2OS cells were transfected by small interfering RNAs (siRNAs) using Lipofectamine RNAi MAX (Invitrogen) according to the manufacturer's instructions with a final concentration of 20 nM siRNA. The siRNAs were purchased from Dharmacon (Lafayette, CO). The target sequence of PRMT1 siRNA was 5′-CGTCAAAG CCAACAAGTTA-3′. A GFP siRNA served as the control with the sequence 5′-AACACUUGUCACUACUUUCUCUU-3′.

Clonogenic assay. A total of 200 to 400 cells were plated on 10-cm dishes and treated with various concentrations of reagents as indicated in the figure legends in duplicate 24 h after plating. For the treatment of U2OS cells with etoposide, the cells were washed twice with phosphate-buffered saline (PBS) after the treatment. The colonies containing approximately 20 or more cells were counted at 10, 12, and 14 days after treatment. For the treatment of immortalized MEFs with blasticidin and OHT, cells were maintained in the medium containing the desired reagents until staining. The cells were allowed to grow for 12 days, and the colonies were fixed and stained with 0.1% crystal violet for 30 min. The stained colonies were counted. The surviving fraction was determined by dividing the average number of colonies for each treatment by the average number of colonies in the control dishes.

Ionizing radiation (IR) treatment. Cells were irradiated at 20 to 24 h after plating at room temperature by using a Theratron T-780 cobalt unit located in the Department of Radiation Oncology at the Jewish General Hospital (Montreal, Quebec, Canada). Doses ranging from 2 to 10 Gy were delivered at a dose rate 0.66 Gy/min. The cells were returned to an incubator after the irradiations and maintained at 37°C for further analysis.

Cell cycle analysis. For all flow cytometry experiments, both cells growing on the surface of the dishes and in the culture medium were harvested, fixed with 75% ethanol, and stored at −20°C for less than 1 week before staining and analysis. All flow cytometry measurements were performed by using FACSCalibur flow cytometer (BD Biosciences). The data were analyzed by using BD CellQuest Pro software. For measurement of BrdU incorporation, cells were incubated with 10 μM BrdU for 45 min before they were harvested. Cells were fixed, washed once with PBS, and treated with 2 M HCl for 20 min. Cells were then neutralized with 0.1 M sodium borate (pH 9.0), washed once with PBS containing 1% bovine serum albumin, and stained with FITC-conjugated anti-BrdU antibody diluted in 100 μl of PBS containing 1% bovine serum albumin and 0.1% Tween 20 (PBS-T) for 20 min. After two washes with PBS-T, cells were resuspended in PBS containing PI at 10 μg/ml and RNase A at 0.2 mg/ml. After 20 to 60 min of incubation, the cells were subjected to flow cytometry analysis. For measurement of phosphorylated histone H3, fixed cells were first stained with anti-phosphohistone H3 (Ser 10) rabbit antibody, and then with FITC-conjugated goat anti-rabbit IgG (Invitrogen) after being washed with dilution buffer (1% fetal bovine serum and 0.1% Triton X-100 in PBS) as described previously (58). Cells were then counterstained with PI. More than 10,000 cells per condition were analyzed by flow cytometry.

Immunofluorescence. Cells growing on glass coverslips were washed with PBS twice and fixed with 4% paraformaldehyde at room temperature for 10 min. The cells were then permeabilized in permeabilization solution (0.5% Triton X-100 in PBS) for 15 min. After three washes with PBS, cells were blocked with 10% goat serum in PBS and stained with mouse anti-γH2AX (1:1,000), rabbit anti-53BP1 (1:200), or rabbit anti-RAD51 (1:20) antibodies diluted in PBS containing 5% goat serum and 0.1% Triton X-100. After three washes, the cells were then stained with Alexa Fluor 488-conjugated goat anti-rabbit and Alexa Fluor 568-

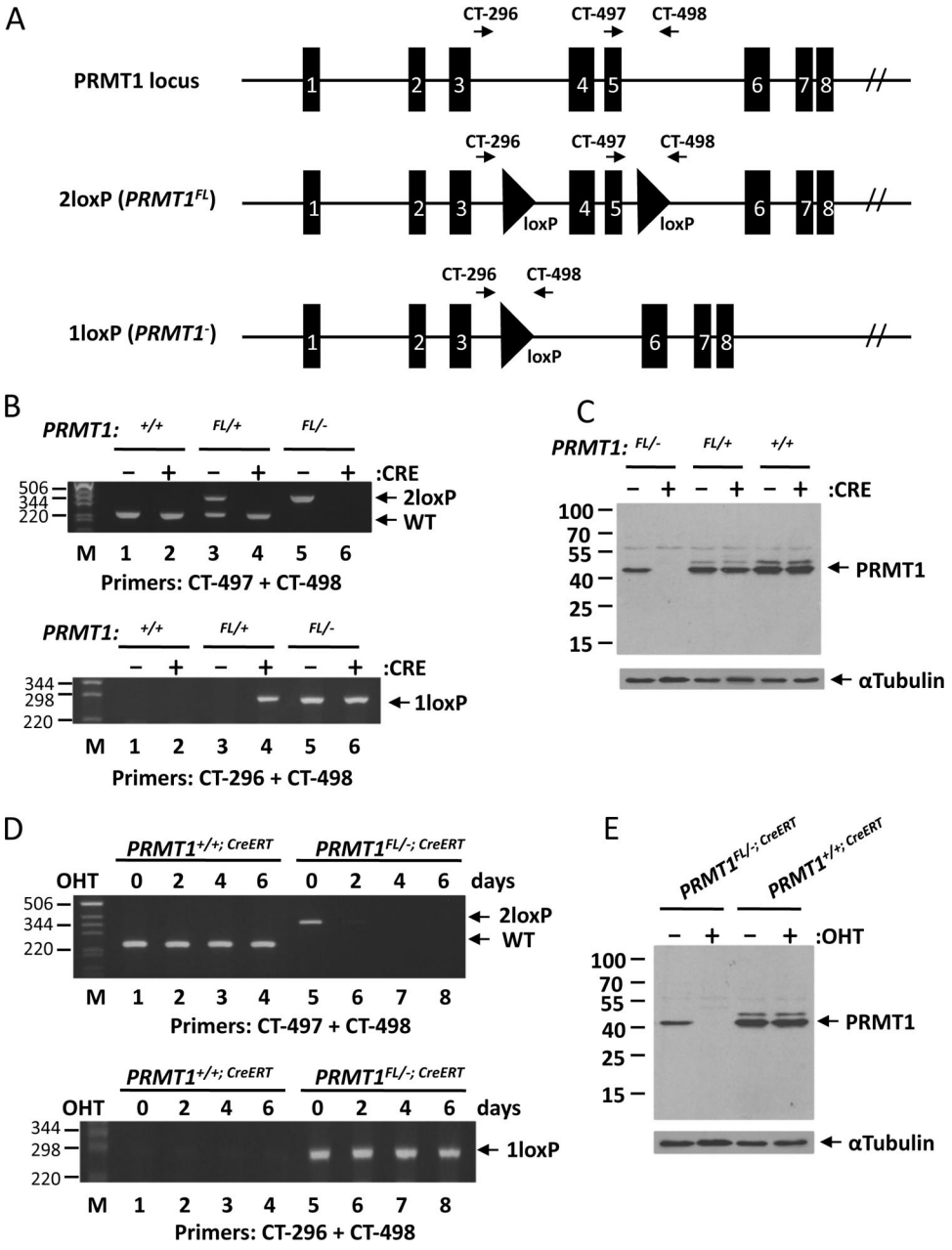

FIG. 1. Generation of a *PRMT1* conditional allele in mice and *PRMT1*-deficient MEFs. (A) Schematic representation of the wild-type (*PRMT1* locus), floxed (2 loxP; $PRMT1^{FL}$), and null (1 loxP; $PRMT1^{-}$) *PRMT1* alleles. The exons are the black boxes, and the line represents introns not drawn to scale. The black triangles denote loxP sites, and the small arrows denote the primers (named CT#) used for PCR analysis. The expected size of the CT-497/498 DNA fragment for the wild-type allele is 245 bp, while the size of the DNA fragment for the 2loxP allele is 358 bp. The expected size of the CT-296/498 DNA fragment after CRE excision is 294 bp. (B) Primary MEFs deficient for PRMT1 were generated by infecting cells with a hygro-CRE retrovirus. Genomic DNA from hygromycin-selected cells was analyzed by PCR, and the DNA fragments were visualized on an ethidium bromide-stained agarose gel. M denotes molecular mass markers of the 1-kb ladder (Invitrogen, Inc.). (C) *PRMT1* MEFs of the indicated genotype infected with hygro-Cre or not were lysed, and the total cellular proteins were analyzed by immunoblotting with anti-PRMT1 and anti-α-tubulin antibodies, as a loading control. The migration of PRMT1 and α-tubulin is shown on the right with arrows, and the migration of the molecular mass markers is shown on the left in kilodaltons. (D) $PRMT1^{FL/-}$ MEFs were immortalized and stably transfected with a plasmid encoding the estrogen receptor-CRE fusion protein (ER-CRE). The cells, termed $PRMT1^{FL/-;CreERT}$ MEFs or control $PRMT1^{+/+;CreERT}$ MEFs, were then treated with OHT for 0, 2, 4, and 6 days, and genomic DNA was isolated and analyzed as in panel B. (E) Total cellular proteins from mock-treated (−) or OHT-treated (+) $PRMT1^{FL/-;CreERT}$ and $PRMT1^{+/+;CreERT}$ MEFs were analyzed by immunoblotting as described for panel C.

conjugated goat anti-mouse secondary antibodies. DNA was counterstained with DAPI (4′,6′-diamidino-2-phenylindole) after three washes with PBS, and coverslips were mounted with Immuno-Mount purchased from Thermo Scientific. Images were taken by using a Zeiss M1 fluorescence microscope.

SKY analysis. The $PRMT1^{FL/-}$ MEFs were left untreated (−OHT) or treated for 4 days with OHT and incubated for another 2 days without OHT (+OHT, 6 days) and analyzed by spectral karyotyping (SKY) at the Banque de Cellules Leucémiques du Québec (Centre de Recherche, Hôpital Maisonneuve-Rose-

mont, Montreal, Quebec, Canada). Slide pretreatment, hybridization with the SkyPaint mouse probes, and detection were performed according to the protocol provided by Applied Spectral Imaging (ASI) with minor modifications. Spectral images were acquired with a SpectraCube system (ASI) mounted on a Zeiss Axioplan II microscope and analyzed using SkyView version 1.6.1 software (ASI). Twenty-four and twenty-eight metaphases were analyzed for the −OHT- and +OHT-treated $PRMT1^{FL/-}$ MEFs.

RESULTS

Generation of *PRMT1* conditional and null alleles in mice. Using the Cre/*loxP* recombination system, we generated a *PRMT1* conditional allele ($PRMT1^{FL}$) that consists of exons 4 and 5 flanked by *loxP* sites. Cre recombinase-mediated deletion of the "floxed" region will remove part of the methyltransferase domain, including the *S*-adenosyl-L-methionine-binding site, and create a frameshift, thereby resulting in a functionally null allele ($PRMT1^{-}$) (Fig. 1A). $PRMT1^{FL/+}$, $PRMT1^{FL/FL}$, and $PRMT1^{+/-}$ mice were grossly normal and fertile, whereas $PRMT1^{-/-}$ embryos did not survive to 7.5 days postcoitum, the earliest time point examined. The role of PRMT1 in embryonic development and adult tissues is under investigation. In the present study, we addressed the cellular function of PRMT1 using MEFs.

PRMT1-deficient MEFs. We isolated MEFs from 14.5-day-postcoitum embryos and generated $PRMT1^{+/+}$ and $PRMT1^{FL/-}$ primary MEFs. To disrupt PRMT1, we infected these primary MEFs with hygromycin-resistant retroviruses that express Cre recombinase (hygro-Cre). The Cre recombinase catalyzed the deletion of the exons between the two loxP sites of $PRMT1^{FL/-}$ allele, resulting in PRMT1-deficient MEFs. PCR amplification of a DNA fragment from genomic DNA isolated from $PRMT1^{FL/-}$ showed that the presence of Cre led to the loss of the DNA fragment for 2loxP and the gain of the 1loxP DNA fragment (Fig. 1B, lanes 4 and 6). Moreover, we stably transfected spontaneously immortalized $PRMT1^{FL/-}$ MEFs with a plasmid encoding the estrogen receptor-CRE fusion protein ($PRMT1^{FL/-;CreERT}$). The addition of OHT for 2, 4, and 6 days led to loss of the 2loxP DNA fragment (Fig. 1D, lanes 6, 7, and 8 [upper panel]), while the 1loxP DNA fragment was observed (Fig. 1D, lanes 5 to 8 [lower panel]). Immunoblotting total cellular extracts from $PRMT1^{FL/-}$ MEFs infected with hygro-Cre retroviruses and $PRMT1^{FL/-;CreERT}$ MEFs treated with OHT showed a complete loss of PRMT1 expression, including the slower-migrating spliced isoform of 48 kDa (Fig. 1C and E) (20). The deletion of exons 4 and 5 is expected to lead to a frameshift and, indeed, we did not observe a truncated protein (Fig. 1C and E). These findings confirm that we have generated a *PRMT1* null allele.

The loss of PRMT1 in MEFs leads to the hypomethylation of cellular proteins, including Sam68 and MRE11. To determine whether PRMT1 is functionally deleted, we immunoblotted total cellular extracts of $PRMT1^{+/+}$ and $PRMT1^{FL/-}$ MEFs with two methylarginine-specific antibodies that recognize proteins with methylated GAR motifs (10). The infection of $PRMT1^{FL/-}$ MEFs with hygro-Cre resulted in hypomethylation of many cellular proteins, as detected with ASYM24 (Fig. 2A) and ASYM25B (Fig. 2B). This hypomethylation was not observed in $PRMT1^{+/+}$ MEFs infected with Cre (Fig. 2A and B). To further confirm the deficiency of PRMT1 function, we

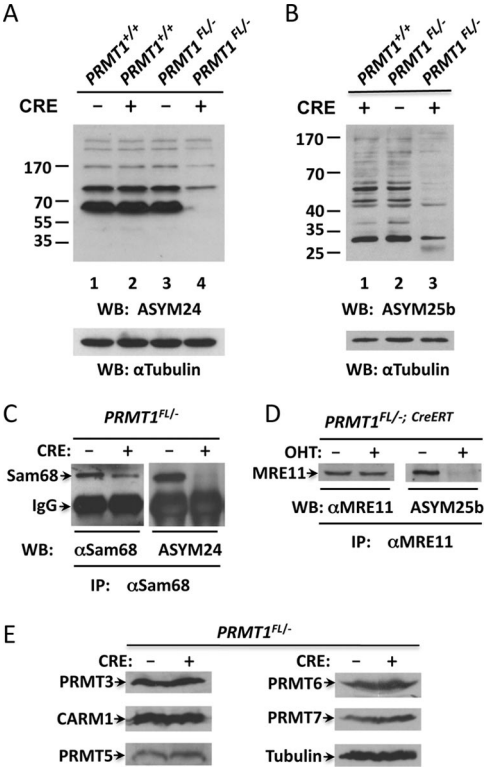

FIG. 2. Hypomethylation of cellular proteins in PRMT1-deficient MEFs. (A and B) $PRMT1^{+/+}$ and $PRMT1^{FL/-}$ MEFs were left untreated (–CRE) or infected with the hygro-Cre retrovirus and selected with hygromycin (+CRE). Cell lysates were immunoblotted with anti-asymmetrical dimethylarginine antibodies ASYM24 (A) or ASYM25b (B) and anti-α-tubulin antibodies to control for equivalent loading. The migration of the molecular mass markers is shown on the left in kilodaltons. (C) $PRMT1^{FL/-}$ MEFs were left untreated (–CRE) or infected with hygro-Cre retroviruses (+CRE) and selected with hygromycin. Whole-cell lysates were immunoprecipitated with anti-Sam68 antibodies. The bound proteins were separated by SDS-polyacrylamide gel electrophoresis and immunoblotted with anti-Sam68 (left panel) and ASYM24 (right panel) antibodies as indicated. The migration of Sam68 and the heavy chain of IgG is shown. (D) $PRMT1^{FL/-;CreERT}$ MEFs were treated with (+OHT) or left untreated (–OHT) for 6 days. Whole-cell lysates were immunoprecipitated with anti-MRE11 antibodies, and the bound proteins were separated by SDS-polyacrylamide gel electrophoresis and immunoblotted with anti-MRE11 and ASYM25b antibodies as indicated. The migration of MRE11 is shown. (E) $PRMT1^{FL/-}$ MEFs were left untreated (–CRE) or infected with hygro-Cre retroviruses (+CRE) and selected with hygromycin. Whole-cell lysates were immunoblotted with the indicated PRMT antibodies or the anti-tubulin antibody to visualize equivalent loading.

immunoprecipitated previously defined PRMT1 substrates, including Sam68 and MRE11, and examined their methylation status. $PRMT1^{FL/-}$ MEFs left untreated or infected with a hygro-CRE retrovirus were immunoprecipitated with anti-Sam68 antibodies and immunoblotted with either anti-Sam68 as control or anti-ASYM24 antibodies to monitor its methylation. The hypomethylation of Sam68 was clearly visible, since the immunoprecipitated Sam68 was not recognized by ASYM24 in the Cre-transduced cells (Fig. 2C). We next utilized $PRMT1^{FL/-;CreERT}$ MEFs treated with OHT for 6 days (+OHT) or left untreated (−OHT). Note that 6 days of OHT treatment means the first 4 days with OHT and the subsequent

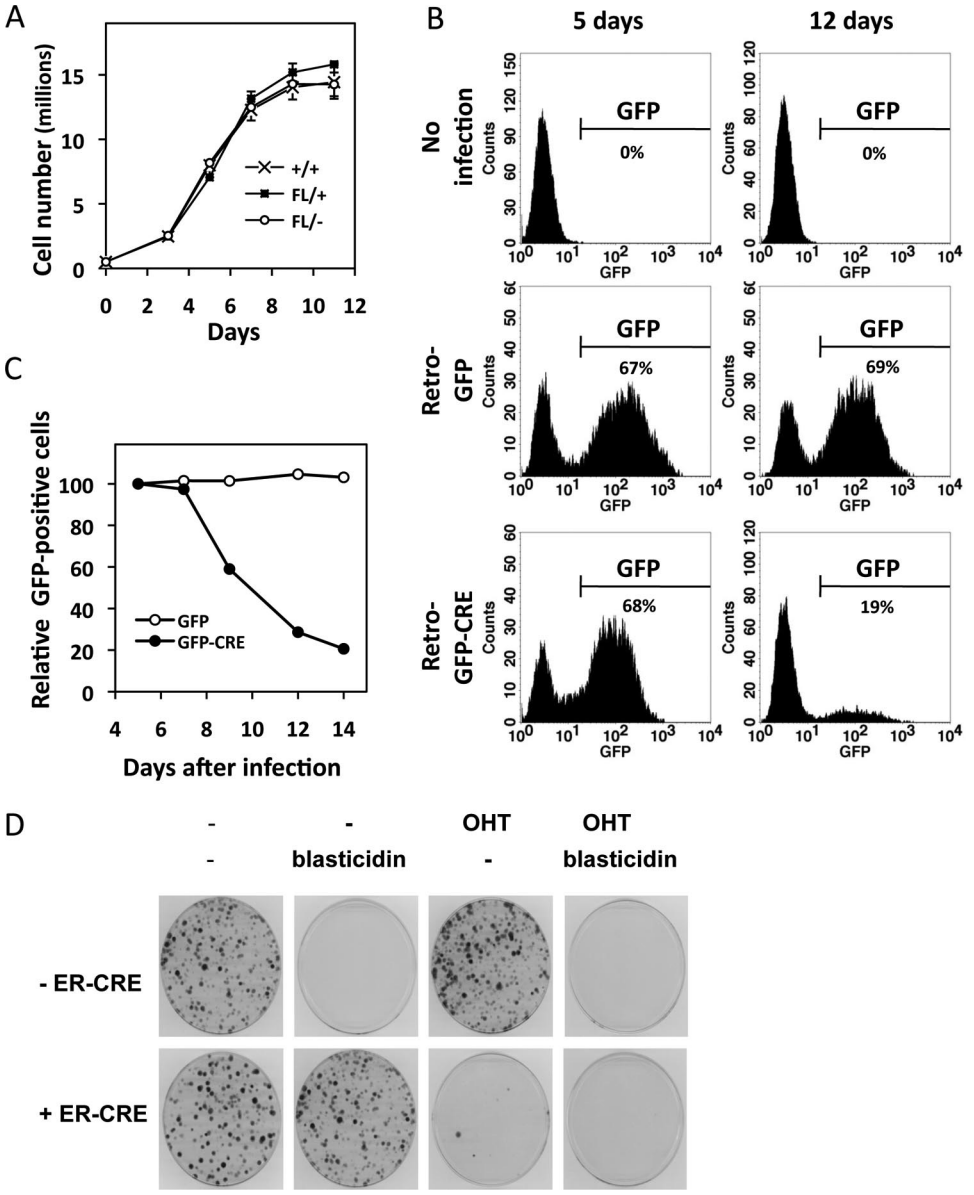

FIG. 3. PRMT1 is essential for the viability of MEFs. (A) The indicated primary PRMT1 MEFs (P3) were plated at cell density of 5×10^5 cells per 10-cm tissue culture dish. Every two or 3 days, the cells were treated with trypsin and counted with a Beckman-Coulter counter, and a quarter of the cells were replated for the next counting ($n = 4$). (B) $PRMT1^{FL/-}$ MEFs were left uninfected (no infection) or infected with retroviruses encoding GFP (GFP) and a GFP-CRE (GFP-CRE) fusion protein, respectively. The GFP-positive cells were identified and counted by flow cytometry at 5 and 12 days postinfection. The *y* axis denotes the cell number, and the *x* axis denotes the GFP fluorescence. (C) The quantification of panel B expressed as a percentage of GFP-positive cells normalized to 100% with day 5. (D) Four hundred $PRMT1^{FL/-}$ (–ER-CRE) and $PRMT1^{FL/-;CreERT}$ (+ER-CRE) MEFs were seeded on 10-cm tissue culture dishes and maintained in regular medium (Dulbecco modified Eagle medium:10% serum) containing different combinations of blasticidin and OHT as indicated. Twelve days later, the cells were fixed, and cell colonies were stained with crystal violet.

2 days without OHT, as described in Materials and Methods. Cell lysates were prepared from OHT-treated cells and immunoprecipitated with anti-MRE11 antibodies. The bound proteins were analyzed by immunoblotting with either anti-MRE11 antibodies as a control or anti-ASYM25b antibodies to monitor its methylation. ASYM25b weakly recognized immunoprecipitated MRE11 from the OHT-treated cells, demonstrating that it is hypomethylated in these cells (Fig. 2D). These results confirm that PRMT1 was functionally deleted from the PRMT1-deficient MEFs, since two of its well-known substrates are hypomethylated. We next immunoblotted with antibodies against other PRMTs, including PRMT3, CARM1 (also known as PRMT4), PRMT5, PRMT6, and PRMT7, to confirm that the loss of PRMT1 does not affect the expression of the other PRMTs. Indeed, the expression of the other PRMTs was not altered with the loss of PRMT1 (Fig. 2E). These findings suggest that the hypomethylation of cellular proteins in PRMT1-deficient

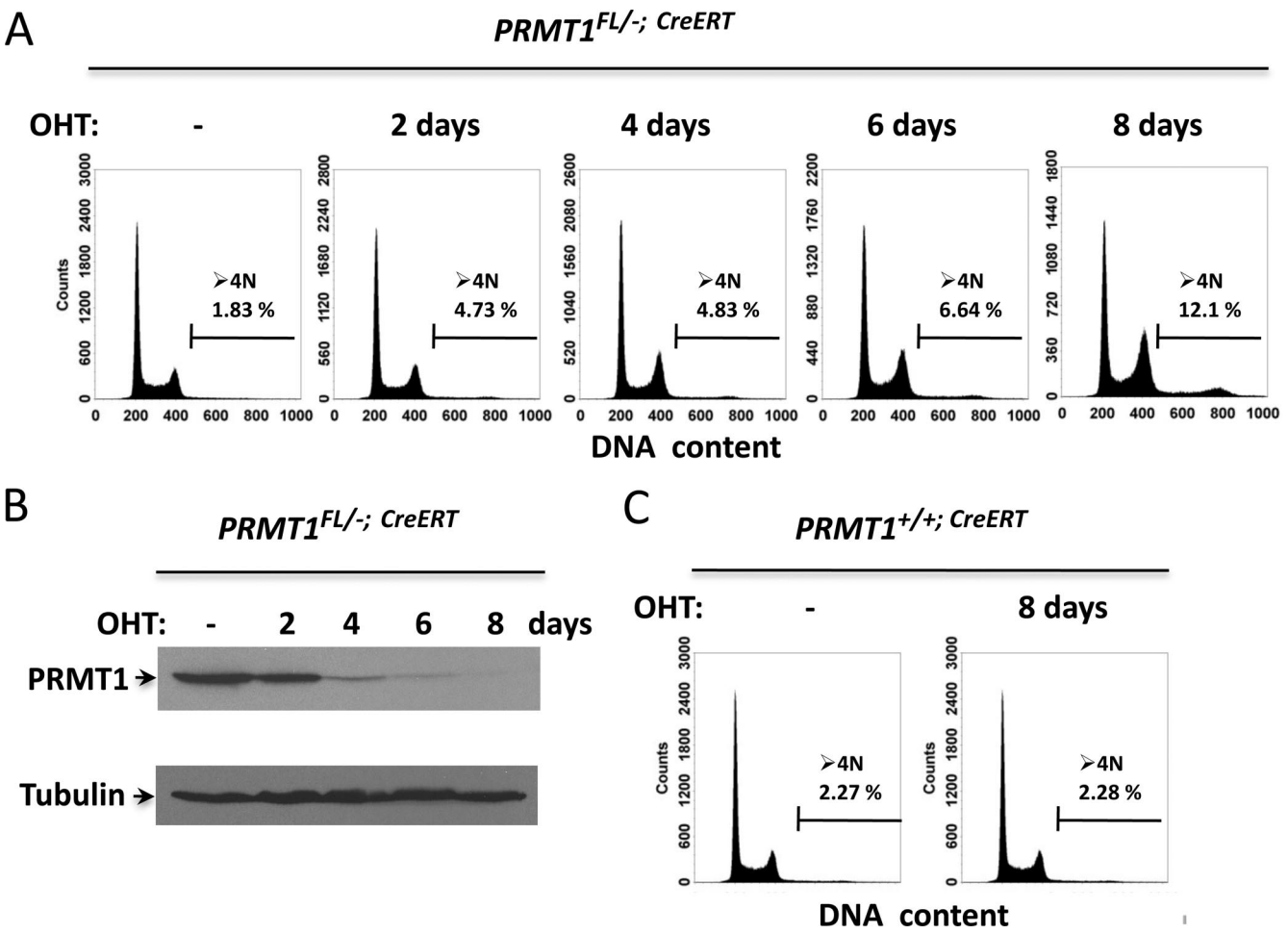

FIG. 4. PRMT1-deficient MEFs exhibit >4N DNA content and accumulation of cells at G_2/M phase. (A) $PRMT1^{FL/-;CreERT}$ MEFs were treated with OHT for the indicated days and the cells were stained with PI and analyzed by cell sorting. The percentage of cells containing >4N DNA content is indicated. The experiments were performed three times, and a representative profile is shown. (B) Cell extracts from OHT-treated $PRMT1^{FL/-;CreERT}$ MEFs were immunoblotted with anti-PRMT1 and antitubulin antibodies to confirm the loss of PRMT1. (C) $PRMT1^{+/+;CreERT}$ MEFs were treated with OHT for the indicated days, and the cells were stained with PI and analyzed by cell sorting. The percentage of cells containing >4N DNA content is indicated.

MEFs is caused by the loss of PRMT1 and not the simultaneous decrease of another PRMT.

The loss of PRMT1 results in cell growth arrest. We initially compared the growth characteristics of primary $PRMT1^{+/+}$, $PRMT1^{FL/+}$, and $PRMT1^{FL/-}$ MEFs. We observed that removal of one allele of PRMT1 did not significantly affect cell proliferation (Fig. 3A). To study the function of PRMT1 in cell proliferation, we infected $PRMT1^{FL/-}$ MEFs with retroviruses that express GFP alone or GFP-CRE and obtained ~70% of the cells to be GFP positive 5 days after infection, as assessed by fluorescence-activated cell sorting (Fig. 3B). However, at 12 days postinfection very few GFP-positive cells remained (~15%) in the Retro-GFP-Cre-infected $PRMT1^{FL/-}$ MEFs (Fig. 3B). These findings suggest that PRMT1 deficiency causes cell death or cell cycle arrest, and thus the cells that were not transfected with CRE overpopulate the PRMT1-deficient slower-growing cells. The GFP-positive cells at day 5 were normalized to 100%, and they were monitored for 2 weeks postinfection for GFP expression and expressed as a percentage. The presence of the Cre recombinase led to ~60% and ~20% survivals of GFP-positive $PRMT1^{FL/-}$ MEFs at 9 and 14 days after retroviral infection, respectively (Fig. 3C). $PRMT1^{FL/-}$ MEFs that were infected with GFP alone survived and maintained their GFP expression (Fig. 3C). These results show that the survival of PRMT1-deficient MEFs may be compromised, suggesting that PRMT1 may be required for the viability of MEFs. To further confirm the requirement of PRMT1 for cell survival and/or proliferation, we next performed a colony formation assay using $PRMT1^{FL/-;CreERT}$ MEFs treated with blasticidin, the antibiotic selection of the CreERT plasmid, and OHT. The generation of PRMT1-deficient cells with ER-CRE (+ER−CRE; blasticidin) and OHT led to no colonies (Fig. 3D). As controls, colonies were obtained with $PRMT1^{FL/-}$ treated with OHT and $PRMT1^{FL/-;CreERT}$ without OHT treatment. These results show that PRMT1-deficient MEFs die or are growth arrested.

PRMT1-deficient MEFs have >4N DNA content and accumulate at the G_2/M phase. To identify the cellular defect(s) of PRMT1-deficient MEFs, we first examined PRMT1 null MEFs for cell cycle defects. We observed that the number of

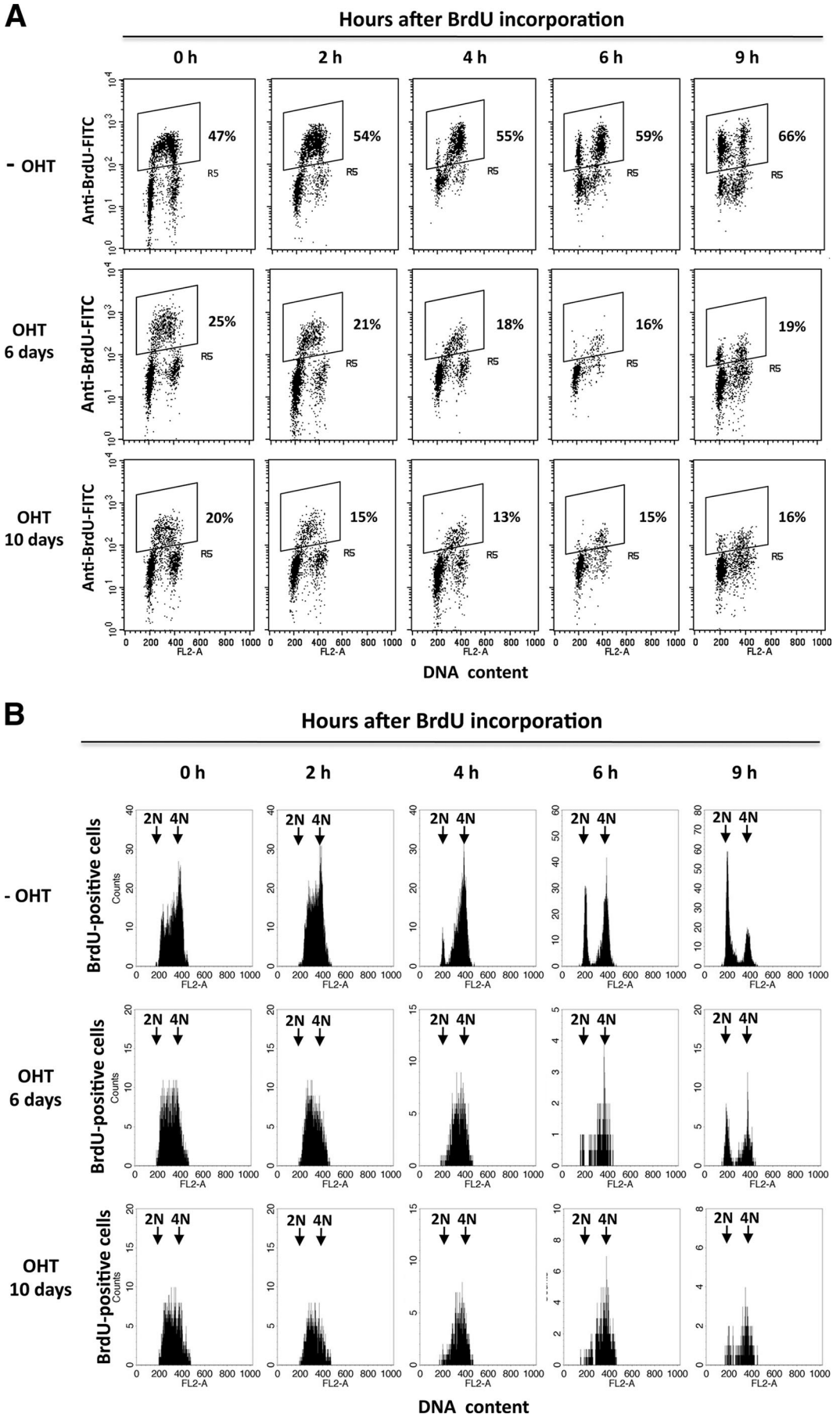
A
Hours after BrdU incorporation
0 h
2 h
4 h
6 h
9 h
- OHT
OHT 6 days
OHT 10 days
Anti-BrdU-FITC
47%
54%
55%
59%
66%
25%
21%
18%
16%
19%
20%
15%
13%
15%
16%
R5
FL2-A
DNA content
B
Hours after BrdU incorporation
BrdU-positive cells
Counts
2N
4N
- OHT
OHT 6 days
OHT 10 days
FL2-A
DNA content

PRMT1$^{FL/-;CreERT}$ MEFs with >4N DNA content gradually increased up to ~12% after 8 days of OHT treatment (Fig. 4A), and this corresponded to the loss of PRMT1 expression, as detected by immunoblotting (Fig. 4B). The OHT treatment did not induce the accumulation of *PRMT1*$^{+/+}$ MEFs at the G_2/M phase, nor did we observe a DNA content >4 N in these cells (Fig. 4C). PRMT1-deficient MEFs did not enter aberrant apoptosis 8 days after OHT treatment, since no significant sub-G_1 peak was observed (Fig. 4A). The absence of substantial cell death and the presence of polyploidy suggest that the loss of PRMT1 results in cells that are growth arrested and polyploid.

PRMT1-deficient MEFs exhibit S-phase reduction and cell cycle delay. To further study the effects of PRMT1 deletion on cell cycle progression, we examined the progression through the S phase using a pulse-chase analysis with BrdU. We treated *PRMT1*$^{FL/-;CreERT}$ MEFs with OHT for 6 and 10 days to generate PRMT1-deficient MEFs. These cells were compared to untreated *PRMT1*$^{FL/-;CreERT}$ MEFs (−OHT). The cells were pulsed with BrdU for 45 min and subsequently chased for 2, 4, 6, and 9 h. In the absence of OHT, at 0 h after BrdU incorporation ~47% of the *PRMT1*$^{FL/-;CreERT}$ MEFs were BrdU positive, and this number increased to ~66% at 9 h after BrdU labeling, a finding consistent with cells cycling (Fig. 5A). In contrast, we observed that *PRMT1*$^{FL/-;CreERT}$ MEFs treated with OHT for 6 and 10 days had a significant decrease in the number of cells in S phase compared to *PRMT1*$^{FL/-;CreERT}$ MEFs without OHT treatment, and this number decreased slightly after BrdU labeling (Fig. 5A). We next examined the ability of the BrdU-positive cells to progress into mitosis and back into the G_0/G_1 phase of the cell cycle. The majority of the BrdU-positive *PRMT1*$^{FL/-;CreERT}$ MEFs without OHT (−OHT) progressed within 4 h to the G_2/M phase of the cell cycle (4N) (Fig. 5B, −OHT), and by 6 h they reached the G_0/G_1 phase (2N) (Fig. 5B, −OHT). In comparison, it took 6 h for BrdU-positive *PRMT1*$^{FL/-;CreERT}$ MEFs with OHT (OHT 6 and 10 days) to progress to the G_2/M phase of the cell cycle. These findings show that PRMT1-deficient MEFs are delayed in cell cycle progression.

***PRMT1*$^{-/-}$ MEFs exhibit spontaneous DNA damage.** The polyploidy and the delayed cell cycle progression suggested that the *PRMT1*$^{-/-}$ MEFs display a phenotype reminiscent of defects in the HR pathway, which also display spontaneous DNA damage, sensitivity to DNA-damaging agents, and checkpoint defects (2). In proliferating cells, DNA double-strand breaks (DSBs) occur mainly during DNA replication and an early marker of DNA damage is the phosphorylation of serine 139 of the histone H2AX variant (γH2AX) (47). To examine whether the *PRMT1*$^{-/-}$ MEFs have spontaneous DNA damage, we counted the number of γH2AX and 53BP1 foci in *PRMT1*$^{FL/-;CreERT}$ MEFs with or without 6 days of OHT treatment (Fig. 6A). We observed that ~30% of the

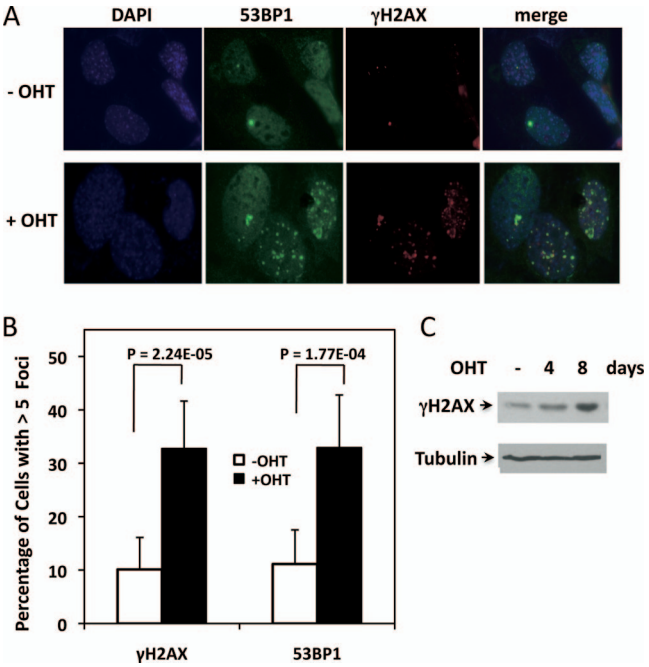

FIG. 6. PRMT1-deficient MEFs exhibit spontaneous DNA damage. (A) *PRMT1*$^{FL/-;CreERT}$ MEFs were left untreated (–OHT) or treated with OHT for 6 days (+OHT). The cells were then visualized by indirect immunofluorescence microscopy using anti-γH2AX and anti-53BP1 antibodies. DAPI staining was used to stain the nucleus. (B) The percentage of cells with >5 foci was counted from three independent experiments. The statistical significance was assessed using the Student *t* test. (C) *PRMT1*$^{FL/-;CreERT}$ MEFs treated for 0, 4, and 8 days with OHT were lysed and analyzed by immunoblotting with anti-γH2AX and antitubulin antibodies.

PRMT1$^{FL/-;CreERT}$ MEFs treated with OHT had >5 γH2AX and >5 53BP1 foci compared to ~10% of the non-OHT treated MEFs, as visualized by indirect immunofluorescence (Fig. 6B). This increase in γH2AX was also observed by immunoblotting after 4 and 8 days OHT treatment (Fig. 6C). These findings show that *PRMT1*$^{-/-}$ MEFs contain increased spontaneous DNA damage.

Loss of PRMT1 leads to genomic instability in MEFs. OHT-treated and nontreated *PRMT1*$^{FL/-;CreERT}$ MEFs were analyzed by SKY. For the definition of the chromosomal abnormalities, the inverted-DAPI banding and spectral images were compared to the SKY-painted chromosomes of the same cell. The most common chromosome number in both cell lines was hypotetraploid and common clonal aberrations, including losses of chromosomes and structural rearrangements that were identified in the two cell lines (Table 1). Representative metaphases are shown in Fig. 7 (see also Fig. S1, S2, and S3 in the supplemental material). We noted that the +OHT cell line

FIG. 5. PRMT1-deficient MEFs exhibit cell cycle delays. (A) *PRMT1*$^{FL/-;CreERT}$ MEFs were left untreated (–OHT) or treated with OHT (OHT 6 and 10 days) to generate PRMT1-deficient MEFs. The cells growing in log phase were incubated with 10 μM BrdU for 45 min, washed twice with complete medium, and then cultured in the absence of BrdU for the indicated times. The experiments were performed twice, and a representative profile is shown. (B) Histogram representation of BrdU-positive cells. The cells from the boxed area of panel A were represented as a histogram. The 2N and 4N DNA is indicated.

TABLE 1. SKY analysis of OHT− and OHT+ MEFs[a]

Clonal abnormality	OHT− cell line	OHT+ cell line
Modal no.	69∼73 (4n-) (24 metaphases/24 analyzed)	65∼79 (4n-) (17 metaphases/28 analyzed)
Chromosome no.		
1		–1 (7 cells)/+Del(1) (2 cells)/+Del(1)x2 (2 cells)
2	**–2** (24 cells)	**–2** (17 cells)
3		–3 (4 cells)/Del(3) (4 cells)
4	**+Del(4)** (3 cells)	–4 (4 cells)/**Del(4)** (3 cells)
5		–5 (4 cells)/Del(5) (3 cells)
6	**Del(6)** (5 cells)/**Del(6)x2** (17 cells)	**Del(6)** (5 cells)/**Del(6)x2** (12 cells)
7	**–7** (19 cells)/–7,–7 (5 cells)	**–7** (15 cells)/Del(7)x2 (2 cells)
8	–8 (3 cells)/**–8,+T(8;2;6;18)** (19 cells)	**–8,+T(8;2;6;18)** (16 cells)
9	–9 (8 cells)/**T(9;18)** (4 cells)/**T(9;18)x2** (17 cells)	**–9** (14 cells)/**T(9;18)** (4 cells)/**T(9;18)x2** (12 cells)
10		–10,–10 (7 cells)
11	**T(11;6;11)** (23 cells)	–11 (5 cells)/**T(11;6;11)** (10 cells)
12		–12 (6 cells)
13	**–13** (20 cells)	**–13** (15 cells)
14		–14 (5 cells)
15	**–15** (13 cells)	**–15** (12 cells)
16	**–16** (24 cells)/**Dic(16;16)** (21 cells)	**–16** (12 cells)/–16,–16 (5 cells)/**Dic(16;16)** (15 cells)
17	**–17** (6 cells)	**–17** (6 cells)
18	**–18** (20 cells)/**T(18;6;8;9)** (5 cells)	**–18** (7 cells)/–18,–18 (7 cells)/**T(18;6;8;9)** (12 cells)
19	**–19** (20 cells)	**–19** (13 cells)/–19,–19 (3 cells)
Single cell abnormalities		
Translocations/other aberrations	Isochromosome 4q, **T(6;18)**, T(8;17), T(8;19)	Dic(1;2), Dic(4;5), Dic(5;7), Dic(11;19), T(1;3), T(1;13), T(1;15), T(3;11), **T(6;18)**, T(7;12), T(9;18;9), T(10;?), T(10;2), T(12;7), T(14;15), T(15;10), +10, +11,+ 14, Del(13), Del(18)
End-to-end fusions (?TAs)	None	(1;4), (1;9), (2;2), (3;3), (5;10), (8;9), (18;18)
Other numerical aberrations	None	42∼59 chromosomes (6 metaphases/28 analyzed); 90∼151 chromosomes (5 metaphases/28 analyzed)

[a] Chromosomal abnormalities were detected by SKY analysis of mouse OHT− and OHT+ cell lines. Clonal chromosomal abnormalities are defined by a chromosome loss in at least three cells and a chromosome gain or a structural rearrangement in at least two cells. All numerical and structural changes are expressed are expressed in relation to the hypotetraploidy level (4n-). T, translocation (the chromosome listed first contains the centromere); Del, deletion; Dic, dicentric; TAs, possible telomeric association. Common abnormalities in OHT− and OHT+ cell lines are indicated in boldface.

had frequent additional aberrations, including a higher incidence of chromosome losses and gains with cells >90 chromosomes (Fig. 7A). The loss of PRMT1 also resulted in the presence of several cells with unique chromosome translocations (Table 1 and Fig. 7B; also see Fig. S3 in the supplemental material). In addition, we noted metaphases with dicentric chromosomes which may suggest end-to-end fusions and with centromeric fusions (Fig. 7B). The presence of 90 to151 chromosomes only in metaphases of the +OHT cell line was observed in 5 of 28 cells, and this shows that the loss of PRMT1 leads to polyploidy. These findings are consistent with cell cycle analysis of Fig. 4 and suggest that the loss of PRMT1 leads to genomic instability.

PRMT1 is required for both the G_2/M and the G_1/S checkpoint activation in response to IR-induced DNA damage. In response to DNA damage, cell cycle checkpoints are activated to arrest cell cycle progression allowing time for repair. The G_1/S checkpoint prevents damaged DNA from being replicated and the G_2/M checkpoint prevents cells from entering mitosis with damaged DNA. We first analyzed the G_1/S checkpoint by measuring the abundance of cells in the S phase 20 h after IR treatment. In the absence of OHT, approximately 47 and 28% of *PRMT1*$^{FL/-;CreERT}$ MEFs entered the S phase of the cell cycle with no treatment and 10 Gy of IR, respectively (Fig. 8A, −OHT). In contrast, 40 and 36% of the OHT-treated *PRMT1*$^{FL/-;CreERT}$ MEFs entered the S phase after no treatment and 10 Gy of IR (Fig. 8A, +OHT). These findings show that *PRMT1*$^{-/-}$ MEFs induced with OHT clearly have lost their S-phase checkpoint and ∼90% of the cells incorporated BrdU after DNA damage (Fig. 8A). An S-phase ratio was obtained for the −OHT- and +OHT-treated samples from two experiments in duplicate, and this ratio closely approaches 1 in PRMT1-deficient cells (+OHT, 0.8), whereas the −OHT MEFs had a ratio close to 0.5, and the difference was significant ($P < 0.05$) (Fig. 8A, lower panels).

We then studied the contribution of PRMT1 to G_2/M checkpoint activation by measuring the abundance of cells entering mitosis 90 min after IR treatment using the anti-phosphorylated S10 histone H3 antibody. Without IR exposure, the frequency of mitotic cells was comparable in OHT-treated and nontreated *PRMT1*$^{FL/-;CreERT}$ MEFs (Fig. 8B) (1.55% versus 1.42%). After 2 Gy of IR treatment, only 25% of the *PRMT1*$^{FL/-;CreERT}$ MEFs progressed to the M phase (from 1.55% to 0.40%), a finding consistent with the majority of wild-type cells arresting before mitosis in the presence of DNA damage. However, 95% of the OHT-treated *PRMT1*$^{FL/-;CreERT}$ MEFs progressed through the M phase (from 1.42% to 1.35%) (Fig. 8B), which is consistent with the cells having lost their G_2/M checkpoint. A mitosis ratio was obtained for the −OHT- and +OHT-treated samples from two experiments in dupli-

FIG. 7. Loss of PRMT1 in MEFs leads to genomic instability by SKY analysis. SKY was performed on the *PRMT1*$^{FL/-;CreERT}$ MEF cells untreated (–OHT) or treated with OHT for 6 days (+OHT). SKY was carried out as described in Materials and Methods. A summary of all chromosomal abnormalities for each cell line is given in Table 1. Two representative metaphase spreads of the +OHT cell line analyzed by SKY are shown. (A) Spectral karyotype of a metaphase with 142 chromosomes, represented in classification pseudocolors. (B) Spectral karyotype of a metaphase with 71 chromosomes. The karyotype is classified with the inverted-DAPI image (left) and the classification pseudocolors (right). Arrows indicate the chromosomal abnormalities that are found only in the +OHT cell line, including unique chromosome deletions and translocations, chromosome breaks, and dicentric chromosomes. The inverted-DAPI image of this metaphase is shown in Fig. S2 in the supplemental material.

cate, and this ratio closely approached 1 in PRMT1-deficient cells (+OHT, 0.9) treated with 2Gy of IR, whereas the −OHT MEFs had a ratio close to 0.3, and the difference was statistically significant ($P < 0.001$) (Fig. 8A, lower panels). The usage of 10 Gy of IR considerably reduced the quantities of cells that stained with antiphosphorylated S10 histone H3 antibody; nevertheless, the difference in the mitosis ratio was statistically significant between the −OHT- and +OHT-treated *PRMT1*$^{FL/-;CreERT}$ MEFs (Fig. 8B, lower panel).

PRMT1-deficient cells are hypersensitive to etoposide treatment. We next examined whether PRMT1-deficient cells were hypersensitive to DNA-damaging agents. We wanted to verify whether PRMT1-deficient cells were hypersensitive to the topoisomerase II inhibitor etoposide, which is known to induce DSBs. Since the *PRMT1*$^{-/-}$ MEFs die within a week or so, we utilized U2OS cells transfected with PRMT1 siRNA to perform a colony formation assay. We reasoned that the PRMT1 deficiency would be required transiently to signal DNA damage, and thus we should not need cells that harbor a stable knockdown of PRMT1. Transient knockdown studies are efficient in the human osteosarcoma cell line U2OS, and these are often used to study the DDR. U2OS cells were transfected with control or PRMT1 siRNA, and the latter cells displayed a reduced level of PRMT1 by ~95%, as observed by immunoblotting using α-tubulin as a loading control (Fig. 9A). The knockdown of PRMT1 in U2OS exhibited a reduced cell growth phenotype consistent with what was observed in MEFs (Fig. 9B).We observed that PRMT1 siRNA-treated U2OS had an increased sensitivity to etoposide-induced DNA damage compared to control siRNA-treated U2OS (Fig. 9C). While control transfected U2OS (siGFP) required a 1 h treatment of 1 μM etoposide to achieve 50% cell death (Fig. 9C, left panel), the siPRMT1 transfected U2OS required a dose lower than 0.5 μM to achieve 50% cell death (Fig. 9C, left panel). Similarly a shorter treatment time (~25 min versus ~50 min) was required to kill 50% of the siPRMT1-transfected U2OS cells with 5 μM etoposide (Fig. 9C, right panel). These findings show that PRMT1-deficient cells are hypersensitive to the DNA-damaging agent etoposide.

Downregulated PRMT1 expression leads to reduced recruitment of RAD51 at sites of DNA damage induced by IR. In proliferating mammalian cells, the major mode of DNA repair is HR (64). One of the key protein complexes is the recombinase protein RAD51, which is essential in repairing DNA DSBs by HR (5). We reasoned that the genomic instability in PRMT1-deficient cells may be caused by a lack or impaired HR. Using anti-RAD51 antibodies, we examined whether the RAD51 recombinase was recruited to DNA damage sites after IR treatment, as detected by focus formation by indirect immunofluorescence. U2OS transfected with PRMT1 siRNA displayed 53BP1 and RAD51 DNA damage foci without exogenous DNA damage, a finding consistent with PRMT1-deficient

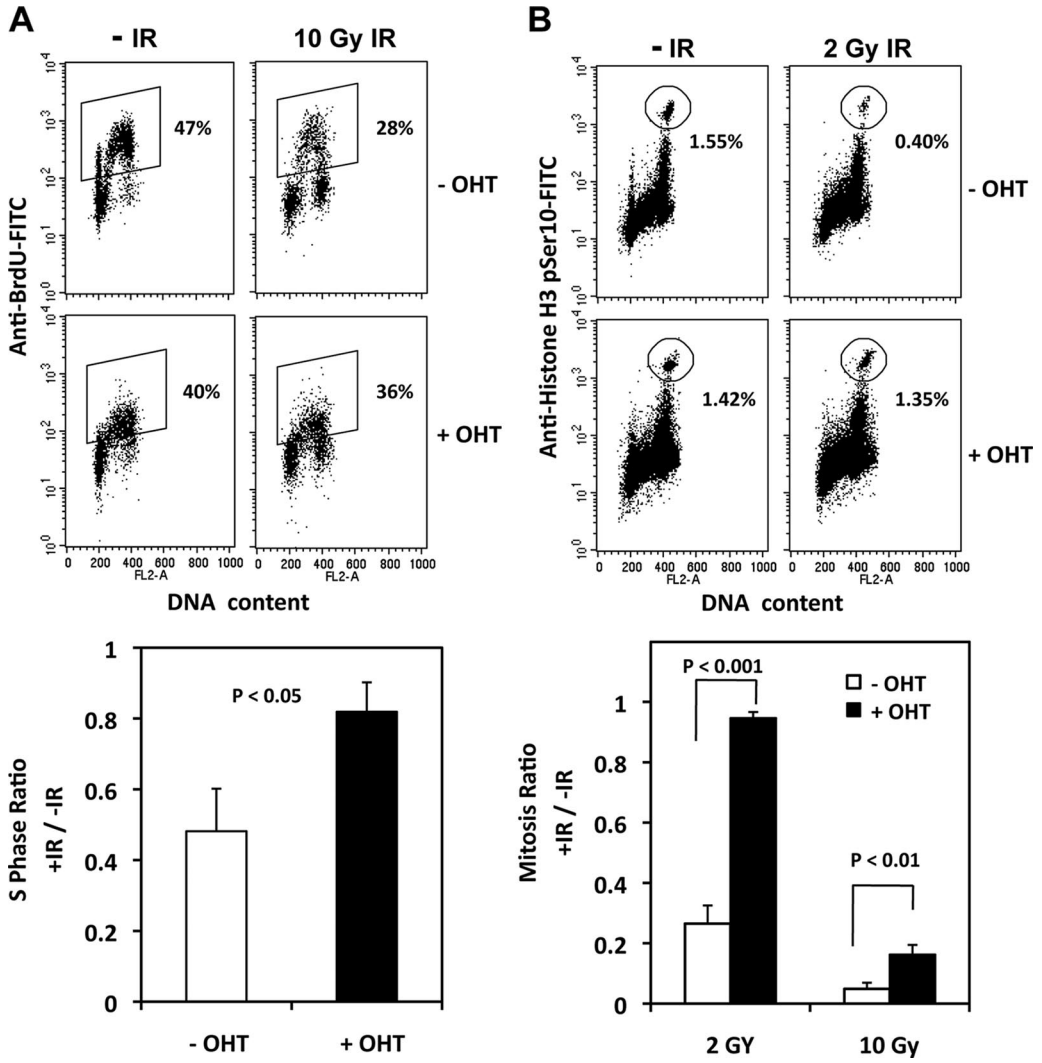

FIG. 8. PRMT1 is required for both the G_2/M and the G_1/S checkpoint activations in response to IR-induced DNA damage. (A) Duplicate cultures of *PRMT1*$^{FL/-;CreERT}$ MEFs were left untreated (–OHT) or treated with OHT (+OHT). One set was treated with 10 Gy of IR (10 Gy IR), and the other set was left untreated (–IR). At 20 h after treatment, the cells were incubated with 10 μM BrdU for 1 h and stained with PI and an FITC-conjugated anti-BrdU antibody. The cells were analyzed by flow cytometry. A typical fluorescence-activated cell sorting profile is shown; the experiments were performed twice in duplicate, and the average is shown. The S-phase ratio was obtained by dividing the percentage of gated BrdU-positive cells treated with 10 Gy of IR by the percentage of gated BrdU-positive cells without IR treatment. Statistical significance was assessed by using Student *t* test. (B) Duplicate cultures of *PRMT1*$^{FL/-;CreERT}$ MEFs were left untreated (–OHT) or treated with OHT (+OHT). One set was treated with 2 Gy of IR (2 Gy IR), and the other set was left untreated (–IR). At 1.5 h after treatment, the cells were fixed and stained with PI and anti-pSer10-histone H3 antibody to identify the cells in mitosis. The percentage of pSer10-histone H3-positive cells (circled area) was determined by flow cytometry. The experiments were performed twice in duplicate. A typical result showing anti-pSer10-histone H3 antibody staining and the M-phase ratio, derived by dividing the percentage gated pSer10-histone H3-positive cells treated with 2 or 10 Gy of IR by the average percentage of gated pSer10-histone H3-positive cells without IR treatment. Statistical significance was assessed by using the Student *t* test.

cells harboring spontaneous DNA damage (Fig. 10). These findings show that RAD51 was able to form foci in PRMT1-deficient cells. We next examined the efficiency by which 53BP1 and RAD51 formed foci in the presence of 10 Gy of IR. The number of cells with >5 foci were counted as a time course of recovery after IR treatment (Fig. 10). 53BP1 foci formed equally well in both siGFP- and siPRMT1-transfected U2OS cells, and the difference was not statistically significant (Fig. 10B, left panel). However, we observed that there was a statistical significant decrease in RAD51 foci that were formed at 2, 6, and 20 h after IR treatment (Fig. 10B, right panel). These findings show that the loss of PRMT1 results in the impairment of IR-induced RAD51 foci.

DISCUSSION

In the present study, we generated a conditional *PRMT1* null allele in mice. Using the Cre/lox-conditional system, we show that the loss of PRMT1 expression leads to the loss of arginine methylation of substrates harboring a GAR motif, including Sam68 and MRE11. PRMT1-deficient cells display genomic instability and cell growth arrest. Furthermore, the cells exhib-

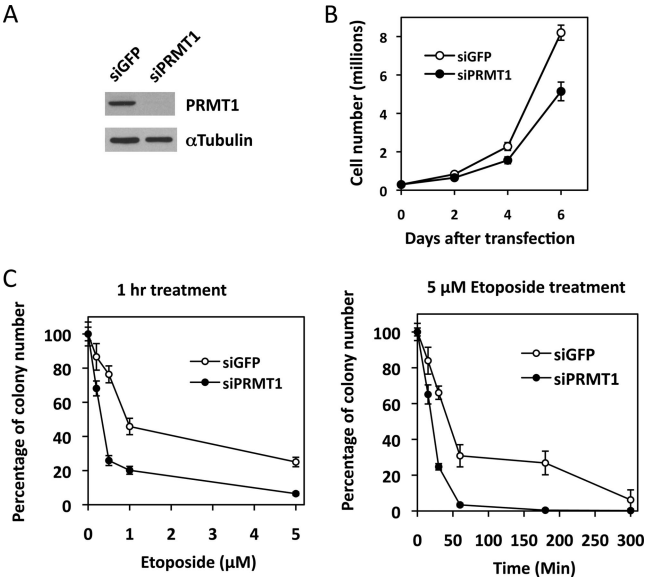

FIG. 9. U2OS cells with downregulated PRMT1 expression are hypersensitive to etoposide treatment. (A) U2OS cells were transfected with siPRMT1 and control siGFP, and the loss of PRMT1 expression was verified by immunoblotting. (B) U2OS cells were plated at 3×10^5 cells/10-cm tissue culture dish and transfected with either siGFP or siPRMT1. The cell growth was monitored by counting with a Beckman-Coulter counter ($n = 4$). (C) Two days after transfection, the cells were treated with trypsin and 400 cells were replated on 10-cm tissue culture dishes. The cells were treated next day with etoposide with the desired dosage and time period as indicated. The cells were then washed twice with PBS and grown in regular medium. The visible colonies containing >20 cells were counted at 10, 12, and 14 days after treatment, respectively, and normalized to 100% without the treatment. Ten fields were randomly selected, and the total number of the colonies in the 10 fields was calculated and expressed as a percentage.

ited spontaneous DNA damage, cell cycle progression delay, checkpoint defects, polyploidy, and chromosome instability. Using PRMT1 siRNA in U2OS cells, we further showed that PRMT1-deficient cells are hypersensitive to the DNA-damaging agent etoposide, and the cells exhibit a defect in IR-induced RAD51 recruitment at DNA damage foci. These data show that PRMT1 is required for genome maintenance and cell proliferation and highlight a key role for arginine methylation in the DDR pathway.

A *PRMT1* hypomorphic allele generated by a gene-trapping strategy which maintains partial PRMT1 expression revealed the need for PRMT1 for early embryonic development as the embryos died at ~E6.5 (44). ES cells derived from the *PRMT1* hypomorphic allele harbor numerous hypomethylated proteins, including Sam68 and MRE11 (11, 20). However, these ES cells did not reveal the essential role for PRMT1 in genome maintenance and cell proliferation. Our findings that the loss of PRMT1 in MEFs results in genomic instability and polyploidy suggests that it may be the residual PRMT1 expression in ES cells that maintains cell viability. Alternatively, it is possible that somatic cells such as fibroblasts (i.e., MEFs) are more sensitive to the lack of arginine methylation by PRMT1. *Saccharomyces cerevisiae* contains one homolog of PRMT1, *Hmt*/*Rmt1*; yeasts null for this methyltransferase are viable (28) and exhibit the hypomethylation of RNA-binding proteins (50), and a role in the maintenance of silent chromatin was observed (69).

The role of arginine methylation, and therefore PRMTs, in cell cycle progression and checkpoint activation is not well characterized. The PRMTs are known to methylate histones and in a histone-dependent manner influence the cell cycle (7). PRMT1 has been shown to methylate H4R3 (52, 61) and cooperates with p300/CBP and CARM1 to activate gene expression (3). Leukemia cells containing the MLL-EEN fusion protein recruit PRMT1 in a Sam68-dependent manner to activate the HoxA9 gene (18). The knockdown of PRMT1 in this circumstance prevents leukemia cell growth (18). CARM1 is required for estrogen-induced cell cycle progression in MCF-7 breast cancer cells (26). The loss of PRMT5 using siRNA leads to the inhibition of cell growth of transformed B cells (62), while overexpression of PRMT5 in NIH 3T3 cells leads to the inhibition of cell proliferation (23). The phenotype we observe with the loss of PRMT1 may only be partly explained by H4R3 methylation, since the loss of PRMT1 changes the expression of only a few genes (36; data not shown).

The role of PRMTs in the DDR is also poorly characterized. We showed previously that mutation of the arginines within the GAR motif of MRE11 severely impairs its exonuclease activity but not its complex formation with NSB1 and RAD50 (11). The GAR motif expressed as a GFP fusion in mammalian cells was sufficient to target to DNA damage foci (21), suggesting that arginine methylation may regulate its interaction with DNA or with the recruitment of subsequent proteins for DNA repair (12, 21). We examined RAD51 foci since HR is dependent on the resection of DSBs by MRN (15) and its recruitment to the break should be impaired under these conditions. The reduced formation of RAD51 foci with IR treatment in PRMT1 siRNA-treated U2OS cells suggests that this defect may be contributed in part by the hypomethylation of MRE11. Another DDR protein that is methylated by PRMT1 is 53BP1, and its arginine methylation was shown to impact its ability to associate with DNA (13) and oligomerize (1). Although general methylase inhibitors prevent the formation of 53BP1 foci, the GAR motif is not required to localize 53BP1 to DNA damage sites (13, 46), since this property is dictated mainly by lysine methylated histones and the tandem Tudor domain of 53BP1 (30). Here, we extend these findings and show that the ability of 53BP1 to localize to DNA damage foci is not affected by the loss of PRMT1. The challenges that lie ahead will be to identify other PRMT1 substrate(s) required for genome maintenance and cell proliferation.

PRMT5, PRMT6, and PRMT7 also play a role during DNA damage. PRMT6 was shown to methylate polymerase β; however, the properties of PRMT6-deficient cells were not characterized (22). Interestingly, the reduced expression of PRMT7 sensitizes cancer cells to camptothecin (60), etoposide (8), and DNA-damaging agents (29). These findings suggest that symmetrical dimethylarginine methylation may also regulate the DDR. Recently, PRMT5 was shown to methylate p53 and regulate its ability to induce cell death and p53-dependent gene expression (32).

The molecular and cellular defects observed with the loss of PRMT1 mimic that of proteins involved in the DDR pathway. Hypomorphic alleles and animal models of the MRN complex

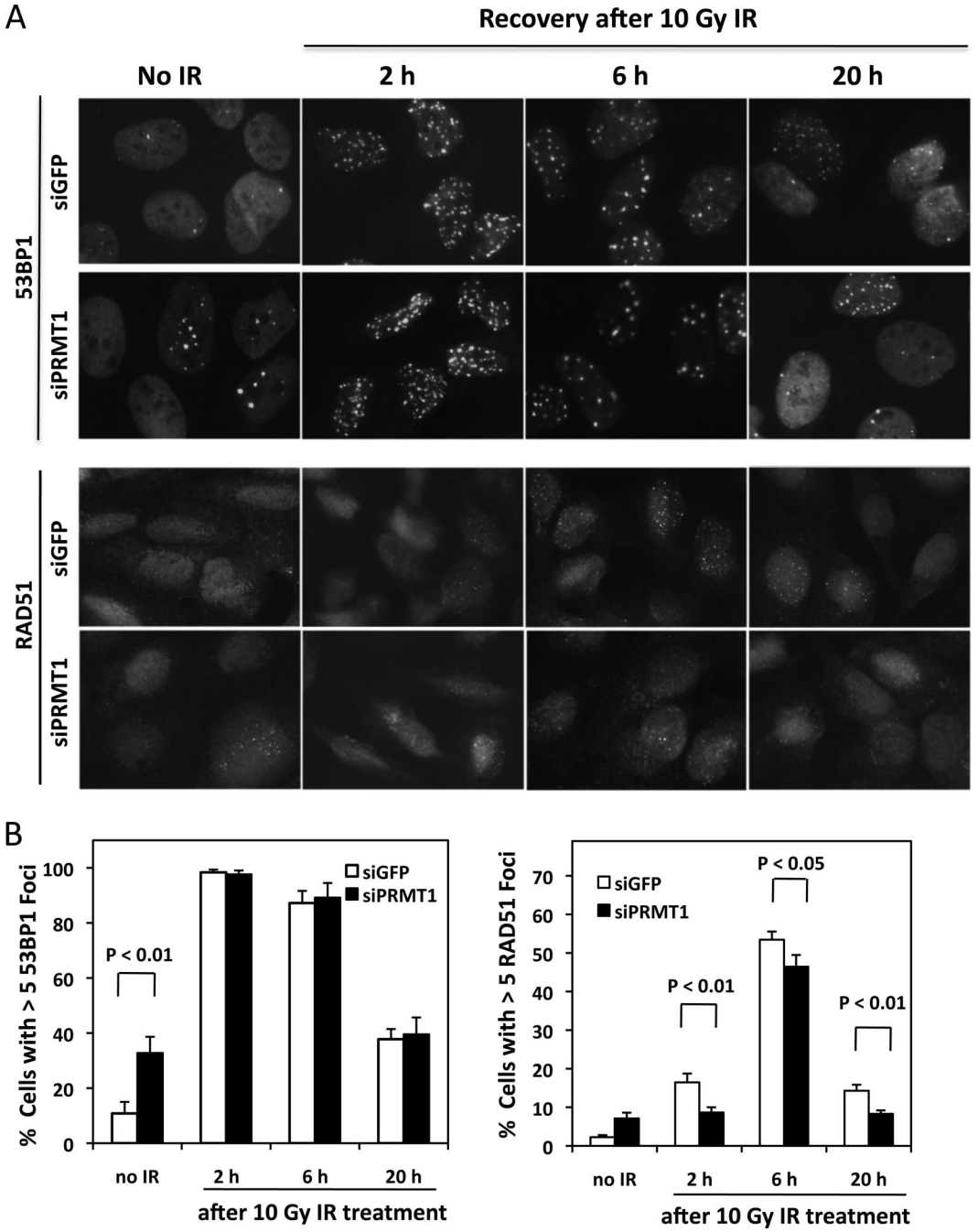

FIG. 10. Downregulation of PRMT1 expression in U2OS cells leads to a reduced recruitment of RAD51 to DNA damage foci after IR treatment. U2OS cells were transfected with control siGFP and siPRMT1 and, 96 h after transfection, the cells were left untreated or treated with 10 Gy of IR. After various hours of recovery, the cells were visualized by indirect immunofluorescence with anti-53BP1 and anti-RAD51 antibodies. (A) Representative images. (B) Cells with >5 foci were counted and are expressed as a percentage. The graphs show the average and standard error of the mean from two independent experiments performed in duplicates where >10 different fields were analyzed. In total, more than 200 cells were counted for each sample in each experiment. Statistical significance was assessed by using the Student *t* test.

display spontaneous DNA damage, hypersensitivity to DNA damage, checkpoint activation defects, and DNA repair defects (2, 15, 31, 34, 51, 57, 63). In proliferating cells, the loss of components required for HR repair, including ATR (14), MRE11 (15, 57), RAD50 (2), NBS1 (34, 63), and RAD51 (59), lead to genomic instability and cell death. Our findings that PRMT1-deficient cells have spontaneous DNA damage, have checkpoint defects, are hypersensitive to DNA-damaging agents, show chromosome instability, and are impaired in recruiting RAD51 to DNA damage sites induced by IR suggest that PRMT1 is a key player in the DDR pathway. Interestingly, the loss of PRMT1 induces polyploidy in the absence of

apoptosis and this is similar to certain Myc mutants (24). Therefore, the loss of PRMT1 may have two separate activities: one related to the cell survival as recently reported (67) and the other via the induction of genomic instability. The result is a polyploid growth arrested cell with increased level of damaged genomic DNA. In PRMT1-deficient cells, we observed cell cycle delays that may suggest checkpoint activation. It remains to be determined whether the low doses of spontaneous DNA damage are responsible of this observation. Recently, it was shown that the loss of a component of the MRN complex, RAD50, in postmitotic tissues is dispensable (2). These findings suggest that the loss of PRMT1 may, like that of RAD50, be tolerated in postmitotic cells and suggest that PRMT1 may represent an important target for cancer treatment.

ACKNOWLEDGMENTS

We thank Hui Su and Jeffrey Bajko for technical assistance and Claude Rondeau (Leukemia Cell Bank of Quebec) for technical assistance in spectral karyotyping. We also thank Guy Sauvageau for providing retroviral vectors. We thank Jean-Yves Masson and Xu-Dong Zhu for helpful discussions. We are grateful to Tom Nicholson and members of the laboratory for critically reading the manuscript.

This study was supported by grant MOP-93811 from the Canadian Institutes of Health Research and the Canadian Cancer Society Research Institute. J.H. is supported by a grant from the Cancer Research Network of Fonds de la Recherche en Santé du Québec. S.R. is a Chercheur-National of the Fonds de la Recherche en Santé du Québec.

REFERENCES

1. **Adams, M. M., B. Wang, Z. Xia, J. C. Morales, X. Lu, L. A. Donehower, D. A. Bochar, S. J. Elledge, and P. B. Carpenter.** 2005. 53BP1 oligomerization is independent of its methylation by PRMT1. Cell Cycle **4:**1854–1861.
2. **Adelman, C. A., S. De, and J. H. Petrini.** 2009. Rad50 is dispensable for the maintenance and viability of post-mitotic tissues. Mol. Cell. Biol. **29:**483–492.
3. **An, W., J. Kim, and R. G. Roeder.** 2004. Ordered cooperative functions of PRMT1, p300, and CARM1 in transcriptional activation by p53. Cell **117:** 735–748.
4. **Bachand, F.** 2007. Protein arginine methyltransferases: from unicellular eukaryotes to humans. Eukaryot. Cell **6:**889–898.
5. **Baumann, P., and S. West.** 1998. Role of the human RAD51 protein in homologous recombination and double-stranded-break repair. Trends Biochem. Sci. **23:**247–251.
6. **Bedford, M. T.** 2007. Arginine methylation at a glance. J. Cell Sci. **120:**4243–4246.
7. **Bedford, M. T., and S. Richard.** 2005. Arginine methylation an emerging regulator of protein function. Mol. Cell **18:**263–272.
8. **Bleibel, W. K., S. Duan, R. S. Huang, E. O. Kistner, S. J. Shukla, X. Wu, J. A. Badner, and M. E. Dolan.** 2009. Identification of genomic regions contributing to etoposide-induced cytotoxicity. Hum. Genet. **125:**173–180.
9. **Boisvert, F. M., J. Côté, M. C. Boulanger, P. Cléroux, F. Bachand, C. Autexier, and S. Richard.** 2002. Symmetrical dimethylarginine methylation is required for the localization of SMN in Cajal bodies and pre-mRNA splicing. J. Cell Biol. **159:**957–969.
10. **Boisvert, F. M., J. Côté, M. C. Boulanger, and S. Richard.** 2003. A proteomic analysis of arginine-methylated protein complexes. Mol. Cell Proteomics **2:**1319–1330.
11. **Boisvert, F. M., U. Déry, J. Y. Masson, and S. Richard.** 2005. Arginine methylation of MRE11 by PRMT1 is required for DNA damage checkpoint control. Genes Dev. **19:**671–676.
12. **Boisvert, F. M., M. J. Hendzel, J. Y. Masson, and S. Richard.** 2005. Methylation of MRE11 regulates its nuclear compartmentalization. Cell Cycle **4:**981–989.
13. **Boisvert, F. M., A. Rhie, S. Richard, and A. J. Doherty.** 2005. The GAR motif of 53BP1 is arginine methylated by PRMT1 and is necessary for 53BP1 DNA binding activity. Cell Cycle **4:**1834–1841.
14. **Brown, E. J., and D. Baltimore.** 2003. Essential and dispensable roles of ATR in cell cycle arrest and genome maintenance. Genes Dev. **17:**615–628.
15. **Buis, J., Y. Wu, Y. Deng, J. Leddon, G. Westfield, M. Eckersdorff, J. M. Sekiguchi, S. Chang, and D. O. Ferguson.** 2008. Mre11 nuclease activity has essential roles in DNA repair and genomic stability distinct from ATM activation. Cell **135:**85–96.
16. **Chen, D., H. Ma, H. Hong, S. S. Koh, S. M. Huang, B. T. Schurter, D. W. Aswad, and M. R. Stallcup.** 1999. Regulation of transcription by a protein arginine methyltransferase. Science **284:**2174–2177.
17. **Chen, T., S. Hevi, F. Gay, N. Tsujimoto, T. He, B. Zhang, Y. Ueda, and E. Li.** 2007. Complete inactivation of DNMT1 leads to mitotic catastrophe in human cancer cells. Nat. Genet. **39:**391–396.
18. **Cheung, N., L. C. Chan, A. Thompson, M. L. Cleary, and C. W. So.** 2007. Protein arginine-methyltransferase-dependent oncogenesis. Nat. Cell Biol. **9:**1208–1215.
19. **Cook, J. R., J. H. Lee, Z. H. Yang, C. D. Krause, N. Herth, R. Hoffmann, and S. Pestka.** 2006. FBXO11/PRMT9, a new protein arginine methyltransferase, symmetrically dimethylates arginine residues. Biochem. Biophys. Res. Commun. **342:**472–481.
20. **Côté, J., F. M. Boisvert, M. C. Boulanger, M. T. Bedford, and S. Richard.** 2003. Sam68 RNA binding protein is an in vivo substrate for protein arginine *N*-methyltransferase 1. Mol. Biol. Cell **14:**274–287.
21. **Déry, U., Y. Coulombe, A. Rodrigue, A. Stasiak, S. Richard, and J. Y. Masson.** 2008. A glycine-arginine domain in control of the human MRE11 DNA repair protein. Mol. Cell. Biol. **28:**3058–3069.
22. **El-Andaloussi, N., T. Valovka, M. Toueille, R. Steinacher, F. Focke, P. Gehrig, M. Covic, P. O. Hassa, P. Schar, U. Hubscher, and M. O. Hottiger.** 2006. Arginine methylation regulates DNA polymerase beta. Mol. Cell **22:** 51–62.
23. **Fabbrizio, E., S. El Messaoudi, J. Polanowska, C. Paul, J. R. Cook, J.-H. Lee, V. Nègre, M. Rousset, S. Pestka, A. LeCam, and C. Sardet.** 2002. Negative regulation of transcription by the type II arginine methyltransferase PRMT5. EMBO Rep. **3:**641–645.
24. **Fest, T., V. Mougey, V. Dalstein, M. Hagerty, D. Milette, S. Silva, and S. Mai.** 2002. c-MYC overexpression in Ba/F3 cells simultaneously elicits genomic instability and apoptosis. Oncogene **21:**2981–2990.
25. **Frankel, A., N. Yadav, J. Lee, T. L. Branscombe, S. Clarke, and M. T. Bedford.** 2002. The novel human protein arginine N-methyltransferase PRMT6 is a nuclear enzyme displaying unique substrate specificity. J. Biol. Chem. **277:**3537–3543.
26. **Frietze, S., M. Lupien, P. A. Silver, and M. Brown.** 2008. CARM1 regulates estrogen-stimulated breast cancer growth through up-regulation of E2F1. Cancer Res. **68:**301–306.
27. **Ganesh, L., T. Yoshimoto, N. C. Moorthy, W. Akahata, M. Boehm, E. G. Nabel, and G. J. Nabel.** 2006. Protein methyltransferase 2 inhibits NF-κB function and promotes apoptosis. Mol. Cell. Biol. **26:**3864–3874.
28. **Gary, J. D., W. J. Lin, M. C. Yang, H. R. Herschman, and S. Clarke.** 1996. The predominant protein-arginine methyltransferase from *Saccharomyces cerevisiae*. J. Biol. Chem. **271:**12585–12594.
29. **Gros, L., C. Delaporte, S. Frey, J. Decesse, B. R. de Saint-Vincent, L. Cavarec, A. Dubart, A. V. Gudkov, and A. Jacquemin-Sablon.** 2003. Identification of new drug sensitivity genes using genetic suppressor elements: protein arginine *N*-methyltransferase mediates cell sensitivity to DNA-damaging agents. Cancer Res. **63:**164–171.
30. **Huyen, Y., O. Zgheib, R. A. Ditullio, Jr., V. G. Gorgoulis, P. Zacharatos, T. J. Petty, E. A. Sheston, H. S. Mellert, E. S. Stavridi, and T. D. Halazonetis.** 2004. Methylated lysine 79 of histone H3 targets 53BP1 to DNA double-strand breaks. Nature **432:**406–411.
31. **International Nijmegen Breakage Syndrome Study Group.** 2000. Nijmegan breakage syndrome. Arch. Dis. Child. **82:**400–406.
32. **Jansson, M., S. T. Durant, E. C. Cho, S. Sheahan, M. Edelmann, B. Kessler, and N. La Thangue.** 2008. Arginine methylation regulates the p53 response. Nat. Cell Biol. **10:**1431–1439.
33. **Jones, B., H. Su, A. Bhat, H. Lei, J. Bajko, S. Hevi, G. A. Baltus, S. Kadam, H. Zhai, R. Valdez, S. Gonzalo, Y. Zhang, E. Li, and T. Chen.** 2008. The histone H3K79 methyltransferase Dot1L is essential for mammalian development and heterochromatin structure. PLoS Genet. **4:**e1000190.
34. **Kang, J., R. T. Bronson, and Y. Xu.** 2002. Targeted disruption of NBS1 reveals its role in mouse development and DNA repair. EMBO J. **21:**1447–1455.
35. **Kim, J., J. Lee, N. Yadav, Q. Wu, C. Carter, S. Richard, E. Richie, and M. T. Bedford.** 2004. Loss of CARM1 results in hypomethylation of thymocyte cyclic AMP-regulated phosphoprotein and deregulated early T-cell development. J. Biol. Chem. **279:**25339–25344.
36. **Kleinschmidt, M. A., G. Streubel, B. Samans, M. Krause, and U. M. Bauer.** 2008. The protein arginine methyltransferases CARM1 and PRMT1 cooperate in gene regulation. Nucleic Acids Res. **36:**3202–3213.
37. **Lee, J., J. Sayegh, J. Daniel, S. Clarke, and M. T. Bedford.** 2005. PRMT8, a new membrane-bound tissue-specific member of the protein arginine methyltransferase family. J. Biol. Chem. **280:**32890–32896.
38. **Le Romancer, M., I. Treilleux, N. Leconte, Y. Robin-Lespinasse, S. Sentis, K. Bouchekioua-Bouzaghou, S. Goddard, S. Gobert-Gosse, and L. Corbo.** 2008. Regulation of estrogen rapid signaling through arginine methylation by PRMT1. Mol. Cell **31:**212–221.
39. **Lin, W. J., J. Gary, M. C. Yang, S. Clarke, and H. R. Herschman.** 1996. The mammalian immediate-early TIS21 protein and the leukemia-associated BTG1 protein interact with a protein-arginine N-methyltransferase. J. Biol. Chem. **271:**15034–15044.

40. **Mallette, F. A., M. F. Gaumont-Leclerc, and G. Ferbeyre.** 2007. The DNA damage signaling pathway is a critical mediator of oncogene-induced senescence. Genes Dev. **21:**43–48.
41. **Miranda, T. B., M. Miranda, A. Frankel, and S. Clarke.** 2004. PRMT7 is a member of the protein arginine methyltransferase family with a distinct substrate specificity. J. Biol. Chem. **279:**22902–22907.
42. **Obianyo, O., T. C. Osborne, and P. R. Thompson.** 2008. Kinetic mechanism of protein arginine methyltransferase 1. Biochemistry **47:**10420–10427.
43. **Ostareck-Lederer, A., D. H. Ostareck, K. P. Rucknagel, A. Schierhorn, B. Moritz, S. Huttelmaier, N. Flach, L. Handoko, and E. Wahle.** 2006. Asymmetric arginine dimethylation of heterogeneous nuclear ribonucleoprotein K by protein-arginine methyltransferase 1 inhibits its interaction with c-Src. J. Biol. Chem. **281:**11115–11125.
44. **Pawlak, M. R., C. A. Scherer, J. Chen, M. J. Roshon, and H. E. Ruley.** 2000. Arginine *N*-methyltransferase 1 is required for early postimplantation mouse development, but cells deficient in the enzyme are viable. Mol. Cell. Biol. **20:**4859–4869.
45. **Pollack, B. P., S. V. Kotenko, W. He, L. S. Izotova, B. L. Barnoski, and S. Pestka.** 1999. The human homologue of the yeast proteins Skb1 and Hsl7p interacts with Jak kinases and contains protein methyltransferase activity. J. Biol. Chem. **274:**31531–31542.
46. **Pryde, F., S. Khalili, K. Robertson, J. Selfridge, A. M. Ritchie, D. W. Melton, D. Jullien, and Y. Adachi.** 2005. 53BP1 exchanges slowly at the sites of DNA damage and appears to require RNA for its association with chromatin. J. Cell Sci. **118:**2043–2055.
47. **Rogakou, E. P., D. R. Pilch, A. H. Orr, V. S. Ivanova, and W. M. Bonner.** 1998. DNA double-stranded breaks induce histone H2AX phosphorylation on serine 139. J. Biol. Chem. **273:**5858–5868.
48. **Rupnik, A., M. Grenon, and N. Lowndes.** 2008. The MRN complex. Curr. Biol. **18:**R455–R457.
49. **Scott, H. S., S. E. Antonarakis, M. D. Lalioti, C. Rossier, P. A. Silver, and M. F. Henry.** 1998. Identification and characterization of two putative human arginine methyltransferases (HRMT1L1 and HRMT1L2). Genomics **48:** 330–340.
50. **Shen, E., M. Henry, V. Weiss, S. Valentini, P. Silver, and M. Lee.** 1998. Arginine methylation facilitates the nuclear export of hnRNP proteins. Genes Dev. **12:**679–691.
51. **Stewart, G. S., R. S. Maser, T. Stankovic, D. A. Bressan, M. I. Kaplan, N. G. Jaspers, A. Raams, P. J. Byrd, J. H. Petrini, and A. M. Taylor.** 1999. The DNA double-strand break repair gene hMRE11 is mutated in individuals with an ataxia-telangiectasia-like disorder. Cell **99:**577–587.
52. **Strahl, B. D., S. D. Briggs, C. J. Brame, J. A. Caldwell, S. S. Koh, H. Ma, R. G. Cook, J. Shabanowitz, D. F. Hunt, M. R. Stallcup, and C. D. Allis.** 2001. Methylation of histone H4 at arginine 3 occurs in vivo and is mediated by the nuclear receptor coactivator PRMT1. Curr. Biol. **11:**996–1000.
53. **Swiercz, R., D. Cheng, D. Kim, and M. T. Bedford.** 2007. Ribosomal protein rpS2 is hypomethylated in PRMT3-deficient mice. J. Biol. Chem. **282:**16917–16923.
54. **Tang, J., P. N. Kao, and H. R. Herschman.** 1998. PRMT3 a type I protein arginine *N*-methyltransferase that differs from PRMT1 in its oligomerization, subcellular localization, substrate specificity, and regulation. J. Biol. Chem. **273:**16935–16945.
55. **Tang, J., P. N. Kao, and H. R. Herschman.** 2000. Protein-arginine methyltransferase I, the predominant protein-arginine methyltransferase in cells, interacts with and is regulated by interleukin enhancer-binding factor 3. J. Biol. Chem. **275:**19866–19876.
56. **Teyssier, C., H. Ma, R. Emter, A. Kralli, and M. R. Stallcup.** 2005. Activation of nuclear receptor coactivator PGC-1α by arginine methylation. Genes Dev. **19:**1466–1473.
57. **Theunissen, J. W., M. I. Kaplan, P. A. Hunt, B. R. Williams, D. O. Ferguson, F. W. Alt, and J. H. Petrini.** 2003. Checkpoint failure and chromosomal instability without lymphomagenesis in Mre11(ATLD1/ATLD1) mice. Mol. Cell **12:**1511–1523.
58. **Theunissen, J. W., and J. H. Petrini.** 2006. Methods for studying the cellular response to DNA damage: influence of the Mre11 complex on chromosome metabolism. Methods Enzymol. **409:**251–284.
59. **Tsuzuki, T., Y. Fujii, K. Sakumi, Y. Tominaga, K. Nakao, M. Sekiguchi, A. Matsushiro, Y. Yoshimura, and T. Morita.** 1996. Targeted disruption of the Rad51 gene leads to lethality in embryonic mice. Proc. Natl. Acad. Sci. USA **93:**6236–6240.
60. **Verbiest, V., D. Montaudon, M. T. Tautu, J. Moukarzel, J. P. Portail, J. Markovits, J. Robert, F. Ichas, and P. Pourquier.** 2008. Protein arginine *N*-methyltransferase 7 (PRMT7) as a potential target for the sensitization of tumor cells to camptothecins. FEBS Lett. **582:**1483–1489.
61. **Wang, H., Z.-Q. Huang, L. Xia, Q. Feng, H. Erdjument-Bromage, B. D. Strahl, S. D. Briggs, C. D. Allis, J. Wong, P. Tempst, and Y. Zhang.** 2001. Methylation of histone H4 at arginine 3 facilitates transcriptional activation by nuclear hormone receptor. Science **293:**853–857.
62. **Wang, L., S. Pal, and S. Sif.** 2008. Protein arginine methyltransferase 5 suppresses the transcription of the RB family of tumor suppressors in leukemia and lymphoma cells. Mol. Cell. Biol. **28:**6262–6277.
63. **Williams, B. R., O. K. Mirzoeva, W. F. Morgan, J. Lin, W. Dunnick, and J. H. Petrini.** 2002. A murine model of Nijmegen breakage syndrome. Curr. Biol. **12:**648–653.
64. **Wyman, C., and R. Kanaar.** 2006. DNA double-strand break repair: all's well that ends well. Annu. Rev. Genet. **40:**363–383.
65. **Yadav, N., D. Cheng, S. Richard, M. Morel, V. R. Iyer, C. M. Aldaz, and M. T. Bedford.** 2008. CARM1 promotes adipocyte differentiation by coactivating PPARγ. EMBO Rep. **9:**193–198.
66. **Yadav, N., J. Lee, J. Kim, J. Shen, M. C. Hu, C. M. Aldaz, and M. T. Bedford.** 2003. Specific protein methylation defects and gene expression perturbations in coactivator-associated arginine methyltransferase 1-deficient mice. Proc. Natl. Acad. Sci. USA **100:**6464–6468.
67. **Yamagata, K., H. Daitoku, Y. Takahashi, K. Namiki, K. Hisatake, K. Kako, H. Mukai, Y. Kasuya, and A. Fukamizu.** 2008. Arginine methylation of FOXO transcription factors inhibits their phosphorylation by Akt. Mol. Cell **32:**221–223.
68. **Yoshimoto, T., M. Boehm, M. Olive, M. F. Crook, H. San, T. Langenickel, and E. G. Nabel.** 2006. The arginine methyltransferase PRMT2 binds RB and regulates E2F function. Exp. Cell Res. **312:**2040–2053.
69. **Yu, M. C., D. W. Lamming, J. A. Eskin, D. A. Sinclair, and P. A. Silver.** 2006. The role of protein arginine methylation in the formation of silent chromatin. Genes Dev. **20:**3249–3254.
70. **Zhang, X., and X. Cheng.** 2003. Structure of the predominant protein arginine methyltransferase PRMT1 and analysis of its binding to substrate peptides. Structure **11:**509–520.